

**Scattered-Field FDTD and PSTD Algorithms with CPML  
Absorbing Boundary Conditions for Light Scattering by  
Aerosols**

by Wenbo Sun, Gordon Videen, QiangFu, and Yongxiang Hu

ARL-RP-0483

July 2014

This is a reprint from *Journal of Quantitative Spectroscopy & Radiative Transfer* 131 (2013) 166–174.

## **NOTICES**

### **Disclaimers**

The findings in this report are not to be construed as an official Department of the Army position unless so designated by other authorized documents.

Citation of manufacturer's or trade names does not constitute an official endorsement or approval of the use thereof.

Destroy this report when it is no longer needed. Do not return it to the originator.

# Army Research Laboratory

Adelphi, MD 20783-1197

---

---

ARL-RP-0483

July 2014

## Scattered-Field FDTD and PSTD Algorithms with CPML Absorbing Boundary Conditions for Light Scattering by Aerosols

Wenbo Sun

Science Systems and Applications, Inc., Hampton, VA 23666

Gorden Videen

Computational and Information Sciences Directorate, ARL

QiangFu

Department of Atmospheric Sciences, University of Washington, Seattle, WA 98195

Yongxiang Hu

NASA Langley Research Center, Hampton, VA 23681

This is a reprint from *Journal of Quantitative Spectroscopy & Radiative Transfer* 131 (2013) 166–174.

## REPORT DOCUMENTATION PAGE

*Form Approved*  
OMB No. 0704-0188

Public reporting burden for this collection of information is estimated to average 1 hour per response, including the time for reviewing instructions, searching existing data sources, gathering and maintaining the data needed, and completing and reviewing the collection information. Send comments regarding this burden estimate or any other aspect of this collection of information, including suggestions for reducing the burden, to Department of Defense, Washington Headquarters Services, Directorate for Information Operations and Reports (0704-0188), 1215 Jefferson Davis Highway, Suite 1204, Arlington, VA 22202-4302. Respondents should be aware that notwithstanding any other provision of law, no person shall be subject to any penalty for failing to comply with a collection of information if it does not display a currently valid OMB control number.

**PLEASE DO NOT RETURN YOUR FORM TO THE ABOVE ADDRESS.**

<b>1. REPORT DATE (DD-MM-YYYY)</b> July 2014		<b>2. REPORT TYPE</b> Reprint		<b>3. DATES COVERED (From - To)</b>	
<b>4. TITLE AND SUBTITLE</b> Scattered-Field FDTD and PSTD Algorithms with CPML Absorbing Boundary Conditions for Light Scattering by Aerosols				<b>5a. CONTRACT NUMBER</b>	
				<b>5b. GRANT NUMBER</b>	
				<b>5c. PROGRAM ELEMENT NUMBER</b>	
<b>6. AUTHOR(S)</b> Wenbo Sun <sup>a</sup> , GordenVideen <sup>b</sup> , QiangFu <sup>c</sup> , and Yongxiang Hu <sup>d</sup>				<b>5d. PROJECT NUMBER</b>	
				<b>5e. TASK NUMBER</b>	
				<b>5f. WORK UNIT NUMBER</b>	
<b>7. PERFORMING ORGANIZATION NAME(S) AND ADDRESS(ES)</b> U.S. Army Research Laboratory ATTN: RDRL-CIE-S 2800 Powder Mill Road Adelphi, MD 20783-1197				<b>8. PERFORMING ORGANIZATION REPORT NUMBER</b>  ARL-RP-0483	
<b>9. SPONSORING/MONITORING AGENCY NAME(S) AND ADDRESS(ES)</b>				<b>10. SPONSOR/MONITOR'S ACRONYM(S)</b>	
				<b>11. SPONSOR/MONITOR'S REPORT NUMBER(S)</b>	
<b>12. DISTRIBUTION/AVAILABILITY STATEMENT</b> Approved for public release; distribution unlimited.					
<b>13. SUPPLEMENTARY NOTES</b> This is a reprint from <i>Journal of Quantitative Spectroscopy &amp; Radiative Transfer</i> 131 (2013) 166–174. <sup>a</sup> Science Systems and Applications, Inc., Hampton, VA 23666, USA, <sup>b</sup> United States Army Research Laboratory, Adelphi, MD 20783, USA, <sup>c</sup> Department of Atmospheric Sciences, University of Washington, Seattle, WA 98195, USA, <sup>d</sup> NASA Langley Research Center, Hampton, VA 23681, USA					
<b>14. ABSTRACT</b> As fundamental parameters for polarized-radiative-transfer calculations, the single-scattering phase matrix of irregularly shaped aerosol particles must be accurately modeled. In this study, a scattered-field finite-difference time-domain (FDTD) model and a scattered-field pseudo-spectral time-domain (PSTD) model are developed for light scattering by arbitrarily shaped dielectric aerosols. The convolutional perfectly matched layer (CPML) absorbing boundary condition (ABC) is used to truncate the computational domain. It is found that the PSTD method is generally more accurate than the FDTD in calculation of the single-scattering properties given similar spatial cell sizes. Since the PSTD can use a coarser grid for large particles, it can lower the memory requirement in the calculation. However, the Fourier transformations in the PSTD need significantly more CPU time than simple subtractions in the FDTD, and the fast Fourier transform requires a power of 2 elements in calculations, thus using the PSTD could not significantly reduce the CPU time required in the numerical modeling. Furthermore, because the scattered-field FDTD/PSTD equations include incident- wave source terms, the FDTD/PSTD model allows for the inclusion of an arbitrarily incident wave source, including a plane parallel wave or a Gaussian beam like those emitted by lasers usually used in laboratory particle characterizations, etc. The scattered-field FDTD and PSTD light-scattering models can be used to calculate single-scattering properties of arbitrarily shaped aerosol particles over broad size and wavelength ranges.					
<b>15. SUBJECT TERMS</b> Finite-difference time domain, Pseudo-spectral time-domain, Light scattering, Light scattering					
<b>16. SECURITY CLASSIFICATION OF:</b>			<b>17. LIMITATION OF ABSTRACT</b>  UU	<b>18. NUMBER OF PAGES</b>  14	<b>19a. NAME OF RESPONSIBLE PERSON</b> GordenVideen
<b>a. REPORT</b> Unclassified	<b>b. ABSTRACT</b> Unclassified	<b>c. THIS PAGE</b> Unclassified			<b>19b. TELEPHONE NUMBER (Include area code)</b> (301) 394-1871

Contents lists available at [ScienceDirect](#)

# Journal of Quantitative Spectroscopy & Radiative Transfer

journal homepage: [www.elsevier.com/locate/jqsrt](http://www.elsevier.com/locate/jqsrt)

## Scattered-field FDTD and PSTD algorithms with CPML absorbing boundary conditions for light scattering by aerosols

Wenbo Sun <sup>a,\*</sup>, Gorden Videen <sup>b</sup>, Qiang Fu <sup>c</sup>, Yongxiang Hu <sup>d</sup><sup>a</sup> Science Systems and Applications, Inc., Hampton, VA 23666, USA<sup>b</sup> United States Army Research Laboratory, Adelphi, MD 20783, USA<sup>c</sup> Department of Atmospheric Sciences, University of Washington, Seattle, WA 98195, USA<sup>d</sup> NASA Langley Research Center, Hampton, VA 23681, USA

### ARTICLE INFO

#### Article history:

Received 30 November 2012

Received in revised form

1 July 2013

Accepted 10 July 2013

Available online 19 July 2013

#### Keywords:

Finite-difference time domain

Pseudo-spectral time-domain

Light scattering

Aerosol particle

### ABSTRACT

As fundamental parameters for polarized-radiative-transfer calculations, the single-scattering phase matrix of irregularly shaped aerosol particles must be accurately modeled. In this study, a scattered-field finite-difference time-domain (FDTD) model and a scattered-field pseudo-spectral time-domain (PSTD) model are developed for light scattering by arbitrarily shaped dielectric aerosols. The convolutional perfectly matched layer (CPML) absorbing boundary condition (ABC) is used to truncate the computational domain. It is found that the PSTD method is generally more accurate than the FDTD in calculation of the single-scattering properties given similar spatial cell sizes. Since the PSTD can use a coarser grid for large particles, it can lower the memory requirement in the calculation. However, the Fourier transformations in the PSTD need significantly more CPU time than simple subtractions in the FDTD, and the fast Fourier transform requires a power of 2 elements in calculations, thus using the PSTD could not significantly reduce the CPU time required in the numerical modeling. Furthermore, because the scattered-field FDTD/PSTD equations include incident-wave source terms, the FDTD/PSTD model allows for the inclusion of an arbitrarily incident wave source, including a plane parallel wave or a Gaussian beam like those emitted by lasers usually used in laboratory particle characterizations, etc. The scattered-field FDTD and PSTD light-scattering models can be used to calculate single-scattering properties of arbitrarily shaped aerosol particles over broad size and wavelength ranges.

© 2013 Elsevier Ltd. All rights reserved.

### 1. Introduction

Remote-sensing methods to determine aerosol properties, like those developed for the NASA Glory mission [1] require accurate modeling of the polarized solar radiation transferred through the atmosphere composing aerosols. As fundamental parameters for polarized-radiative-transfer calculations, single-scattering phase-matrix elements of irregularly shaped

aerosol particles must be accurately modeled. However, the size parameters of aerosols under the broad solar spectrum generally reside in the range where neither Rayleigh or Rayleigh-Gans, nor geometric optics method can be applied to calculate their light scattering properties. Although for these size parameters exact algorithms such as those based on Mie theory [2] and the *T*-matrix method [3] are very efficient at calculating light scattering from specific, ideal morphologies, like spheres, spheroids, and cylinders, these methods generally have limited applicability to the real-world irregularly shaped aerosol particles. Thus, with the advance of computing resources, numerical light-scattering solutions such as the discrete dipole approximation (DDA) [4–8], the finite-difference time domain (FDTD) technique

\* Correspondence to: Mail Stop 420, NASA Langley Research Center, 21 Langley Boulevard, Hampton, VA 23681-2199, USA. Tel.: +1 757 864 9986.

E-mail addresses: [Wenbo.Sun-1@nasa.gov](mailto:Wenbo.Sun-1@nasa.gov), [w.sun@larc.nasa.gov](mailto:w.sun@larc.nasa.gov) (W. Sun).

[9–16] and the pseudo-spectral time-domain (PSTD) method [17–23] are used more and more frequently in light-scattering studies.

The FDTD technique is formulated by replacing temporal and spatial derivatives in Maxwell's equations with their finite-difference equivalences. To ensure numerical stability and accurate calculation, the finite-difference spatial cell sizes are generally set to be  $\lambda_d/20$  to  $\lambda_d/10$ , where  $\lambda_d$  is the wavelength inside the particle. Theoretically, the FDTD is an accurate method for any particle size parameters. However, for large particles, the FDTD's requirement for a small spatial cell size results in formidably large computational memory and CPU time requirements. Therefore, for large electromagnetic structure scattering problems, the PSTD algorithm which could be numerically stable even with a spatial cell size as large as  $\lambda_d/2$  have significant advantages [17], at least in computational memory requirements.

In this study, we develop a scattered-field FDTD light scattering model and a scattered-field PSTD light-scattering model with the convolutional perfectly matched layer (CPML) [15,24] absorbing boundary condition (ABC) to truncate the computational domain, as a supplementary development to the polarized-radiative-transfer model for applications to irregular aerosol particles. Because the scattered-field FDTD/PSTD equations include incident wave source terms, the FDTD/PSTD model allows for the inclusion of an arbitrarily incident wave source, including a plane parallel wave or a Gaussian beam like those emitted by lasers that are often used in laboratory particle characterizations, etc. In Section 2, the FDTD and PSTD light scattering models with the convolutional perfectly matched layer (CPML) absorbing boundary conditions (ABC) are introduced. In Section 3, sample numerical results are shown. Summary and conclusions are given in Section 4.

## 2. Method

### 2.1. Scattered-field finite-difference time domain method

Following our previous study for a light beam's interaction with an arbitrary dielectric surface [16], we applied the scattered-field FDTD technique to calculate light scattering by particles of arbitrary shapes in free space. The scattered-field FDTD method with wave source terms in its update equations allows more flexibility in the specification of the form of the incident fields, which can be either plane parallel wave or a Gaussian beam, etc. [16]. Following [16], in a Cartesian grid system the x components of the scattered magnetic and electric fields in the scattered-field FDTD algorithm, e.g., are in the forms

$$H_x^{s,n+1/2}(i,j+1/2,k+1/2) = H_x^{s,n-1/2}(i,j+1/2,k+1/2) + \frac{\Delta t}{\mu_0 \Delta s} \times \left[ E_y^{s,n}(i,j+1/2,k+1) - E_y^{s,n}(i,j+1/2,k) + E_z^{s,n}(i,j,k+1/2) - E_z^{s,n}(i,j+1,k+1/2) \right], \quad (1a)$$

$$E_x^{s,n+1}(i+1/2,j,k) = \left( \frac{2\varepsilon - \sigma \Delta t}{2\varepsilon + \sigma \Delta t} \right) E_x^{s,n}(i+1/2,j,k) + \left( \frac{2\Delta t / \Delta s}{2\varepsilon + \sigma \Delta t} \right) \left[ H_y^{s,n+1/2}(i+1/2,j,k-1/2) \right.$$

$$\left. - H_y^{s,n+1/2}(i+1/2,j,k+1/2) + H_z^{s,n+1/2}(i+1/2,j+1/2,k) - H_z^{s,n+1/2}(i+1/2,j-1/2,k) \right] - \left( \frac{\sigma \Delta t}{2\varepsilon + \sigma \Delta t} \right) \left[ E_x^{i,n+1}(i+1/2,j,k) + E_x^{i,n}(i+1/2,j,k) \right] - \left( \frac{2\varepsilon - 2\varepsilon_0}{2\varepsilon + \sigma \Delta t} \right) \left[ E_x^{i,n+1}(i+1/2,j,k) - E_x^{i,n}(i+1/2,j,k) \right], \quad (1b)$$

where  $\mu_0$  and  $\varepsilon_0$  are the permeability and permittivity of free space, respectively;  $\varepsilon$  and  $\sigma$  are the permittivity and conductivity of the medium including the scattering particle, respectively;  $\Delta s$  and  $\Delta t$  denote the spatial cell size and time increment, respectively. To guarantee the numerical stability of the FDTD scheme, we use  $\Delta t = \Delta s / (2c)$ , where  $c$  is the light speed in free space. The indices  $(i, j, k)$  denote the center positions of the spatial cells in the FDTD grid. The time step is denoted by integer  $n$ . The positions of the magnetic and electric field components on a spatial cell are identical to those illustrated in Sun et al. [13]. In this study, the incidence field  $E^i$  is set as a continuous wave and analytically given at any grid points where there is dielectric material.

The convolutional perfectly matched layer (CPML) ABC developed by Roden and Gedney [24] is used to truncate the computational domain in the FDTD/PSTD calculations. The CPML is based on the stretched-coordinate form of the perfectly matched layer (PML) [25] and is more accurate than the uniaxial perfectly matched layer (UPML) ABC [26]. The CPML ABC is more efficient and more suitable for truncation of computational domains with generalized materials. For both scattered/total field formulation and purely scattered-field formulation of the FDTD/PSTD, the CPML ABC can be directly applied to truncate the calculated fields even where the incident-wave source exists. For example, to match a CPML along a boundary to a lossy isotropic half-space characterized by permittivity  $\varepsilon$  and conductivity  $\sigma$  in which the fields update equations are given as Eqs. (1a) and (1b), the update equations of  $H_x$  and  $E_x$  in the CPML can be written in the form [15]:

$$H_x^{s,n+1/2}(i,j+1/2,k+1/2) = H_x^{s,n-1/2}(i,j+1/2,k+1/2) - \frac{\Delta t}{\mu_0} \left\{ [E_z^{s,n}(i,j+1,k+1/2) - E_z^{s,n}(i,j,k+1/2)] / [\kappa_y(j+1/2)\Delta s] - [E_y^{s,n}(i,j+1/2,k+1) - E_y^{s,n}(i,j+1/2,k)] / [\kappa_z(k+1/2)\Delta s] \right\} - \frac{\Delta t}{\mu_0} \left[ H_{xy}^{s,n}(i,j+1/2,k+1/2) - H_{xz}^{s,n}(i,j+1/2,k+1/2) \right], \quad (2)$$

where

$$H_{xy}^{s,n}(i,j+1/2,k+1/2) = b_y(j+1/2)H_{xy}^{s,n-1}(i,j+1/2,k+1/2) + c_y(j+1/2)[E_z^{s,n}(i,j+1,k+1/2) - E_z^{s,n}(i,j,k+1/2)] / \Delta s, \quad (3a)$$

$$H_{xz}^{s,n}(i,j+1/2,k+1/2) = b_z(k+1/2)H_{xz}^{s,n-1}(i,j+1/2,k+1/2) + c_z(k+1/2)[E_y^{s,n}(i,j+1/2,k+1) - E_y^{s,n}(i,j+1/2,k)] / \Delta s. \quad (3b)$$

$$E_x^{s,n+1}(i+1/2,j,k) = \left( \frac{2\varepsilon - \sigma \Delta t}{2\varepsilon + \sigma \Delta t} \right) E_x^{s,n}(i+1/2,j,k)$$

$$\begin{aligned}
& + \left( \frac{2\Delta t}{2\varepsilon + \sigma\Delta t} \right) \left\{ \left[ H_z^{s,n+1/2}(i+1/2, j+1/2, k) \right. \right. \\
& - H_z^{s,n+1/2}(i+1/2, j-1/2, k) \left. \right] / [\kappa_y(j)\Delta s] \\
& - \left[ H_y^{s,n+1/2}(i+1/2, j, k+1/2) \right. \\
& \left. - H_y^{s,n+1/2}(i+1/2, j, k-1/2) \right] / [\kappa_z(k)\Delta s] \left. \right\} \\
& + \left( \frac{2\Delta t}{2\varepsilon + \sigma\Delta t} \right) \left[ E_{x,y}^{s,n+1/2}(i+1/2, j, k) \right. \\
& \left. - E_{x,z}^{s,n+1/2}(i+1/2, j, k) \right], \quad (4)
\end{aligned}$$

where

$$\begin{aligned}
E_{x,y}^{s,n+1/2}(i+1/2, j, k) &= b_y(j)E_{x,y}^{s,n-1/2}(i+1/2, j, k) \\
& + c_y(j)[H_z^{s,n-1/2}(i+1/2, j+1/2, k) \\
& - H_z^{s,n-1/2}(i+1/2, j-1/2, k)]/\Delta s, \quad (5a)
\end{aligned}$$

$$\begin{aligned}
E_{x,z}^{s,n+1/2}(i+1/2, j, k) &= b_z(k)E_{x,z}^{s,n-1/2}(i+1/2, j, k) \\
& + c_z(k)[H_y^{s,n-1/2}(i+1/2, j, k+1/2) \\
& - H_y^{s,n-1/2}(i+1/2, j, k-1/2)]/\Delta s. \quad (5b)
\end{aligned}$$

The  $b_y$ ,  $b_z$ ,  $c_y$ ,  $c_z$  in these equations are given in the form ( $u=x, y$ , or  $z$ ):

$$b_u = e^{-\Delta t((\sigma_u/\varepsilon_0\kappa_u)+(a_u/\varepsilon_0))}, \quad (6a)$$

$$c_u = \frac{(b_u-1)\sigma_u}{\sigma_u\kappa_u + \kappa_u^2 a_u} \quad (6b)$$

The CPML properties ( $a_x, \kappa_x, \sigma_x$ ), ( $a_y, \kappa_y, \sigma_y$ ), and ( $a_z, \kappa_z, \sigma_z$ ) are scaled tensor parameters independent of the medium permittivity  $\varepsilon$  and conductivity  $\sigma$ , and are assigned to the FDTD grids in the CPML in the form as [15]

$$a_x = (x/d)^m a_{x,\max}, \quad (7a)$$

$$\kappa_x(x) = 1 + (x/d)^m (\kappa_{x,\max} - 1), \quad (7b)$$

$$\sigma_x(x) = (x/d)^m \sigma_{x,\max}. \quad (7c)$$

where  $x$  is the depth in the CPML and  $d$  is the CPML thickness in this direction. The parameters  $a_{x,\max}$ ,  $\kappa_{x,\max}$  and  $\sigma_{x,\max}$  denote the maximum  $a_x$ ,  $\kappa_x$  and  $\sigma_x$  at the outmost layer of the CPML; e.g., considering an  $x$ -directed plane wave impinging at angle  $\theta$  upon a PEC-backed CPML with polynomial grading material properties, the reflection factor can be derived as [25]

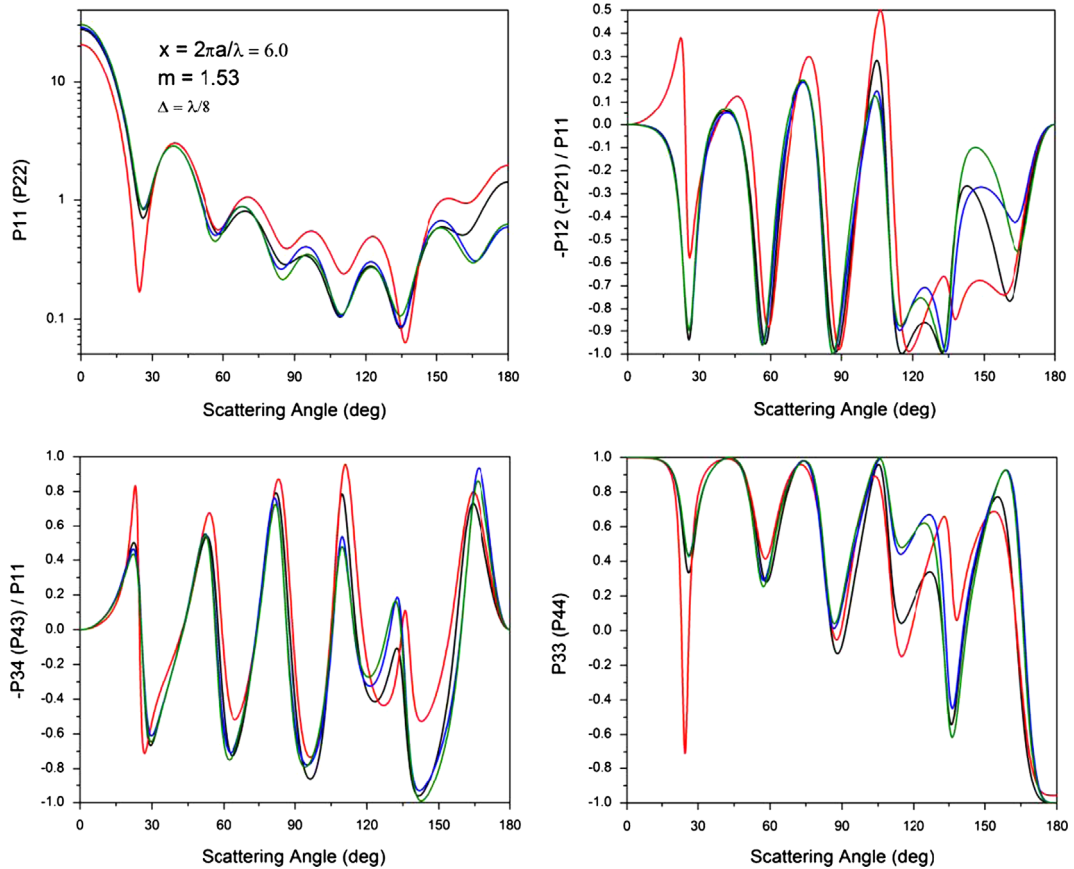


**Fig. 1.** Nonzero light-scattering phase matrix elements from the Lorenz–Mie theory (black), the FDTD (red), the PSTD (blue), and the PSTD with truncation of wavenumbers (olive) for a spherical aerosol particle with a size parameter of  $x=6$  and a refractive index of  $m=1.53$ . In the PSTD and FDTD calculations, the spatial cell size is set as  $1/8$  incident wavelength. (For interpretation of the references to color in this figure legend, the reader is referred to the web version of this article.)

$$R(\theta) = \exp \left[ -\frac{2 \cos \theta}{\epsilon_0 c} \int_0^d \sigma(x) dx \right] = \exp \left[ -\frac{2 \sigma_{x,\max} d \cos \theta}{\epsilon_0 c(m+1)} \right]. \quad (8)$$

Therefore, with a reflection factor  $R(0)$  for normal incidence,  $\sigma_{x,\max}$  can be defined as

$$\sigma_{x,\max} = -\frac{(m+1)\epsilon_0 c \ln [R(0)]}{2d}. \quad (9)$$

As an accurate approach,  $R(0)$  can range from  $10^{-12}$  to  $10^{-5}$ ,  $\kappa_{x,\max}$  and  $a_{x,\max}$  can be chosen with accuracy tests, and the numerical errors are not very sensitive to them. In this study, we choose  $R(0)=10^{-8}$ ,  $\kappa_{x,\max}=1.1$ , and  $a_{x,\max}=0.1$ .

Using the equations reported in this section, a scattered-field formulation of the FDTD that includes the source term can be implemented inside the CPML. The scattered-field CPML FDTD has great flexibility in simulating electromagnetic wave scattering by dielectric particles and surfaces.

The single-scattering properties of particles are calculated with the volume integration of the total electric field in the frequency domain [14]. The total electric field is the superposition of the incident and scattered fields:  $\mathbf{E}=\mathbf{E}^i+\mathbf{E}^s$ . The FDTD simulation is run for  $20N_d$  time steps, where  $N_d$  denotes the spatial cell number in the largest dimension of the computational domain. The frequency

domain correspondent of the total field is obtained from the discrete Fourier transform (DFT) of the time series of the field.

### 2.2. Scattered-field pseudo-spectral time domain method

The spatial discretization in the FDTD method causes dispersion errors, which limit the spatial cell size used in numerical calculations to not larger than 1/20 to 1/10 of the wavelength [13]. Therefore, the FDTD method requires a large number of spatial cells to calculate the light scattering, even by particles of intermediate sizes. The PSTD algorithm was recently developed to avoid this problem, which ideally needs only two spatial cells per wavelength to discretize the computational domain and is free of spatial dispersion errors [17]. The coarse discretization of the PSTD algorithm enables this method to be an optimal solution for large particles. The errors introduced in the PSTD algorithm are claimed to be only the temporal discretization error [18]. For a 3-dimensional (3D) problem, the PSTD requires a stability criterion as [18]

$$\Delta t \leq \frac{2\Delta s}{\sqrt{3}\pi c}, \quad (10)$$

which is a stability criterion with smaller temporal discretization than that of the FDTD. In this study, we set  $\Delta t=\Delta s/(3c)$  for the PSTD calculations.

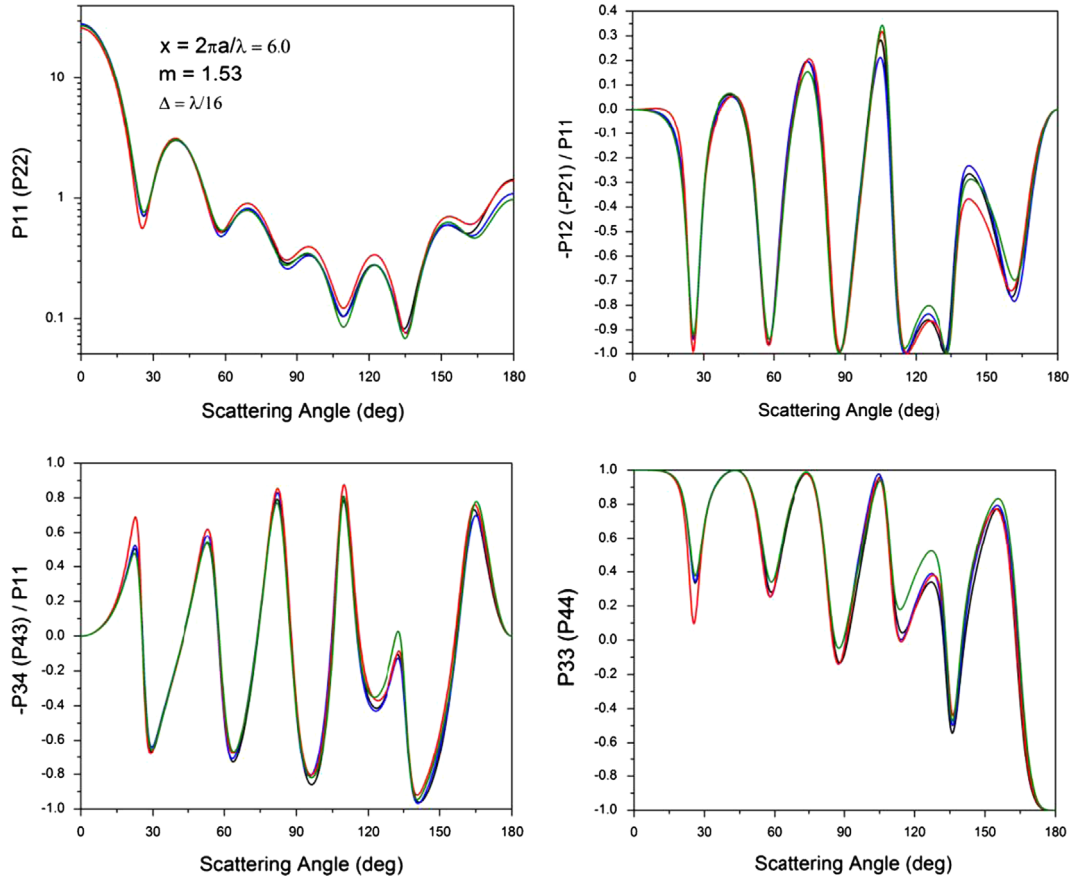


Fig. 2. Same as in Fig. 1, but in the PSTD and FDTD calculations, the spatial cell size is set as 1/16 incident wavelength.

The essence of the PSTD is to use Fourier integrals to obtain the derivative of a field  $f(u)$

$$\begin{aligned} \frac{\partial f(u)}{\partial u} &= \frac{\partial}{\partial u} \left\{ \int_{-\infty}^{\infty} F[f(u)]e^{-iku} dk \right\} \\ &= - \int_{-\infty}^{\infty} ikF[f(u)]e^{-iku} dk = -F^{-1} \{ ikF[f(u)] \}, \end{aligned} \quad (11)$$

where  $u$  denotes a spatial coordinate ( $x, y,$  or  $z$ );  $F$  and  $F^{-1}$  denote the forward and inverse Fourier transforms;  $k$  denotes the wavenumber variable in the Fourier transform; and  $i = \sqrt{-1}$ . This is a well-known formula in mathematics with a long history [27,28].

Based on the scattered-field CPML FDTD method introduced in Section 2.1, we can obtain the scattered-field CPML PSTD algorithm by replacing all the finite-difference approximations of spatial derivatives of fields in the FDTD update equations, including those in the CPML, with the precise spatial derivatives from the Fourier transforms in Eq. (11). Since all the field components are calculated at spatial cell centers in the PSTD algorithm, the spatial position shifts of “+1”, “+1/2”, and “−1/2” in all of the FDTD update equations, including those in the CPML in Section 2.1, are removed for the PSTD field update equations. No other modifications are necessary in this FDTD-to-PSTD modification. The PSTD is run for  $30N_d$  time steps in this study.

Note here that the forward and inverse Fourier transforms are performed using the fast Fourier transform (FFT) and the inverse fast Fourier transform (IFFT) codes given in *Numerical Recipes* [29]. The FFT and IFFT are performed spatially for each time step, along each direction of  $x, y,$  and  $z$ , using the field throughout the whole computational domain, including the CPML, to obtain the spatial derivatives of both electric and magnetic field components at each grid point, prior to the field update calculations.

Our practice shows that the PSTD does avoid the spatial dispersion errors that can cause the FDTD method to become numerically unstable when too few spatial cells are used. However, the PSTD method does have significant numerical errors from different sources, in addition to the errors caused by temporal discretizations as claimed by Liu et al. [18]. The most pronounced error source is the so-called Gibbs phenomenon [18], which involves both the fact that Fourier sums overshoot at a discontinuity, and that this overshoot does not disappear as the frequency increases. For electromagnetic wave propagation in homogeneous media, the PSTD works ideally because there is no Gibbs effect. But for light-scattering problems, a particular medium-and-field-discontinuity case, the Gibbs effect causes significant errors. Since the Fourier transforms in the PSTD algorithm are conducted throughout the whole computational domain at each time step, and the field

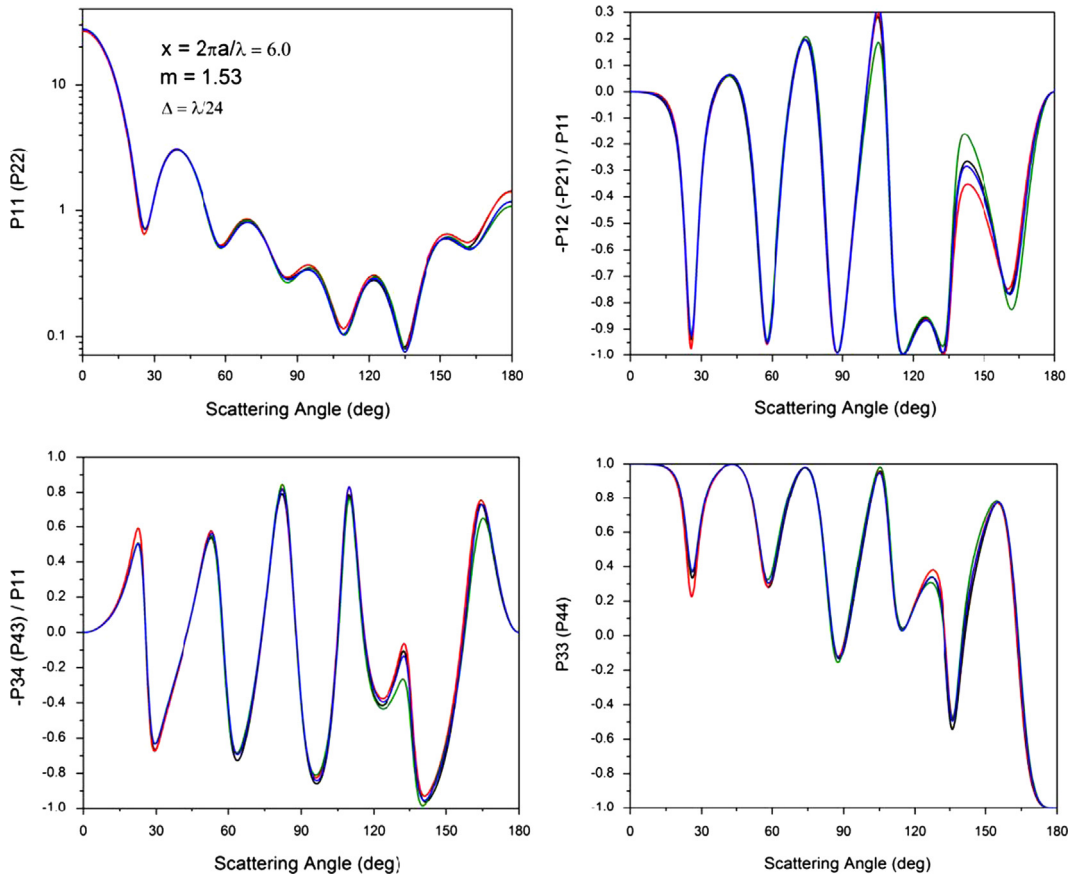


Fig. 3. Same as in Fig. 1, but in the PSTD and FDTD calculations, the spatial cell size is set as 1/24 incident wavelength.

derivatives at each grid point are actually derived from fields throughout the whole computational domain, including those in the CPML, the Fourier transformation errors (Gibbs effect) at any field discontinuity are transmitted everywhere and to every time step. These errors contaminate the whole computational domain and even cause numerical instability of the PSTD method [23]. Liu et al. [18] state that using purely scattered fields in the calculation could decrease the Gibbs effect, and this is also the reason why we use scattered-field FDTD and PSTD algorithm in this study.

### 3. Results

Light scattering is a typical electromagnetic problem with discontinuities. Though the PSTD method is claimed to be a rigorous algorithm without numerical dispersion errors, its Fourier transformation errors (Gibbs effect) due to these discontinuities and finite sums of spectral terms are actually very significant. If there is no special treatment to control these errors, the original PSTD is generally numerically unstable when particle size parameter is large [23]. Using volume-averaged dielectric constant [23] could decrease the discontinuities of the fields, but could also alter the scattering physics at the particle edge. Truncation

of the wavenumbers in the inverse Fourier transformation to eliminate high wavenumber terms [23] can stabilize the PSTD algorithm, but can also cause errors in the numerical results due to the unphysical manipulation of the scattered fields. In this study, we will not average the dielectric constant in both the FDTD and PSTD calculations. To see the errors caused by the wavenumber truncation, we will compare the results from the original PSTD and the PSTD with truncation of the wavenumbers in the inverse Fourier transformation. We choose to truncate 10% of the wavenumbers at the high end in the inverse Fourier transformation for the comparisons in this study.

Fig. 1 shows the nonzero light-scattering phase matrix elements from the Lorenz–Mie theory (black), the FDTD (red), the PSTD (blue), and the PSTD with truncation of wavenumbers (olive) for a spherical aerosol particle with a size parameter of  $x=6$  and a refractive index of  $m=1.53$  for dust aerosols. The reason why we choose non-absorbing particles with large refractive index is that light scattering by these type of particles is the most difficult to be accurately approached by numerical models like the DDA/FDTD/PSTD. If a numerical model is accurate on these particles, it can perform well on aerosols under a wide incident light spectrum. In the PSTD and FDTD calculations in Fig. 1, the spatial cell size is set as  $1/8$  incident

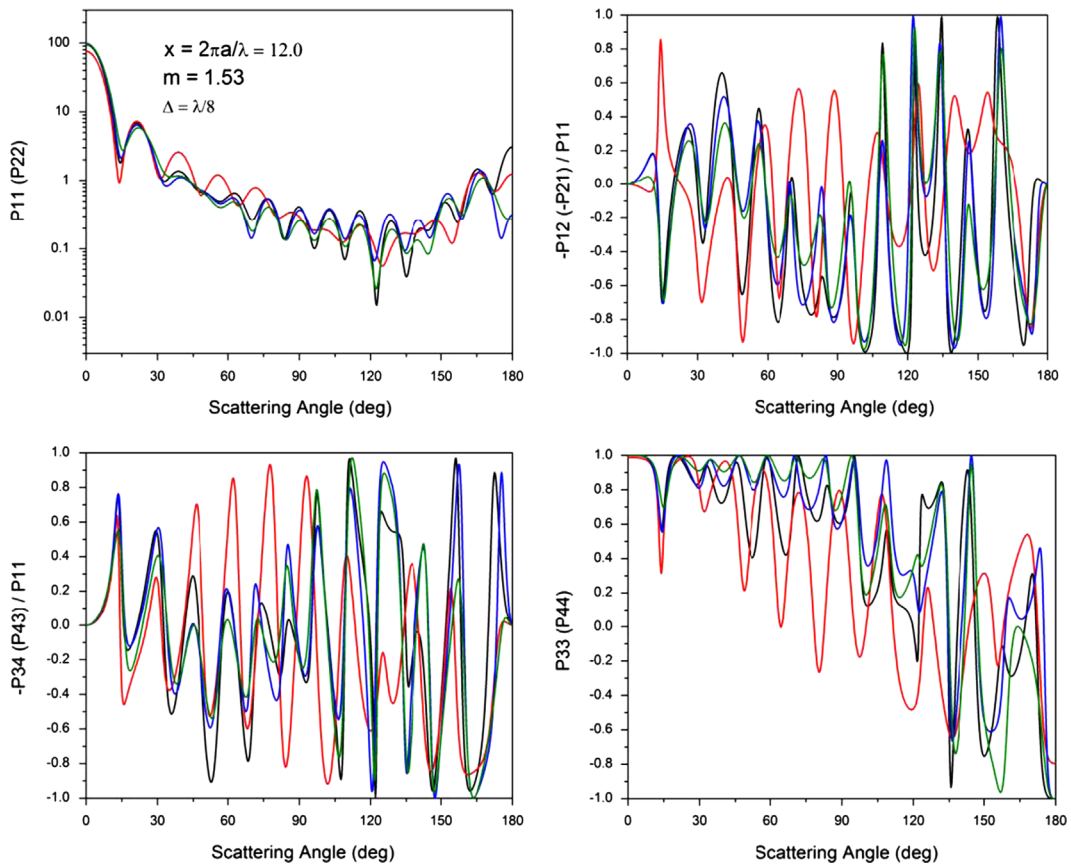


Fig. 4. Nonzero light-scattering phase matrix elements from the Lorenz–Mie theory (black), the FDTD (red), the PSTD (blue), and the PSTD with truncation of wavenumbers (olive) for a spherical aerosol particle with a size parameter of  $x=12$  and a refractive index of  $m=1.53$ . In the PSTD and FDTD calculations, the spatial cell size is set as  $1/8$  incident wavelength. (For interpretation of the references to color in this figure legend, the reader is referred to the web version of this article.)

wavelength. We can see that due to the big spatial cell size of  $1/8$  incident wavelength, the FDTD results in significant numerical dispersion errors in all of the light scattering phase matrix elements. However, the PSTD results generally follow those of the Lorenz–Mie curves, though large errors do exist at many scattering angles. When smaller spatial cell sizes of  $1/16$  and  $1/24$  incident wavelength are used, as shown in Figs. 2 and 3 respectively, the FDTD dispersion errors are greatly reduced. However, the PSTD results are affected by the spatial cell size not as significantly as in the FDTD, as shown in Figs. 2 and 3. This is because the errors of the PSTD are majorly due to Gibbs phenomenon and in nature different from the numerical dispersion errors of the FDTD algorithm. In principle, numerical dispersion errors can be totally removed by infinitely decreasing the spatial cell size, but the Gibbs effect errors of the PSTD cannot. Also, from Figs. 1–3 we can see that truncation of wavenumbers in the inverse Fourier transformation in the PSTD can cause significant errors in the single-scattering phase matrix elements.

For a larger spherical particle with a size parameter of 12 and a refractive index of 1.53, Fig. 4 shows that when the spatial cell size is set as  $1/8$  incident wavelength, the PSTD results for this larger particle generally follow those from the Lorenz–Mie theory, though significant errors exist at most scattering angles; whereas, those from the FDTD are quite different from the exact results due to the

numerical dispersion error of the FDTD method. When smaller spatial cell sizes of  $1/16$  and  $1/24$  incident wavelength are used, as shown in Figs. 5 and 6 respectively, the FDTD errors are greatly reduced, but the PSTD errors are still not significantly changed. For the PSTD, the truncation of wavenumbers cause more significant errors when the spatial cell size is bigger.

The light scattering efficiencies ( $Q_s$ ) and asymmetry factors ( $g$ ) for the cases in Figs. 1–3 and 4–6 are listed in Tables 1 and 2, respectively. We can see that scattering efficiency and the asymmetry parameter from the PSTD are significantly more accurate than those from the FDTD. However, truncation of the wavenumbers in the PSTD can cause large errors in the scattering efficiency and asymmetry parameter.

In summary, the scattered-field FDTD method with the CPML ABC still needs spatial cell sizes of  $\sim \lambda_d/20$  to approach a good accuracy in calculated single-scattering properties. But a spatial cell size of  $\sim \lambda_d/10$  in the PSTD can result in accurate results. So the PSTD is more suitable for calculation of light scattering by larger particles. However, the PSTD has significant Gibbs effect errors which cannot be reduced even by significantly decreasing the spatial cell size, especially for large particles. Also, though the PSTD requires much lower spatial resolution ( $\Delta S \approx \lambda_d/10$ ) than the FDTD ( $\Delta S \approx \lambda_d/20$ ) for an accurate calculation of the single-scattering properties of particles, its two Fourier

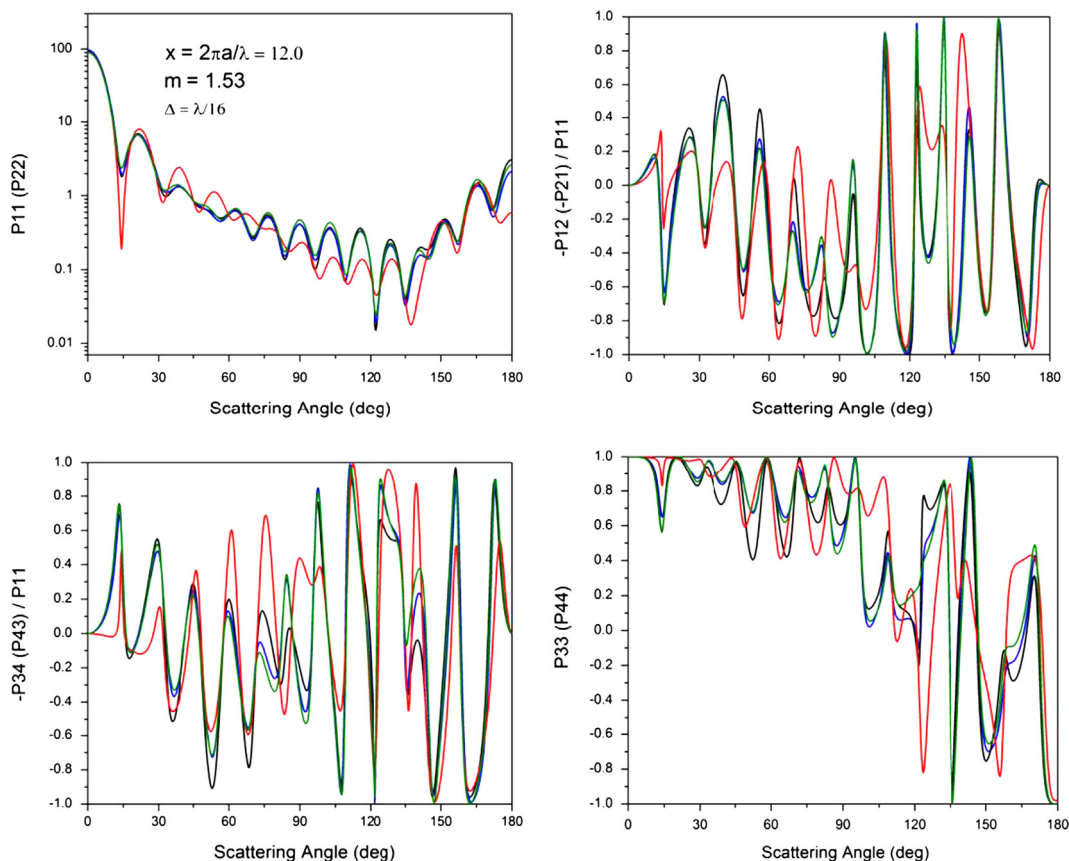


Fig. 5. Same as in Fig. 4, but in the PSTD and FDTD calculations, the spatial cell size is set as  $1/16$  incident wavelength.

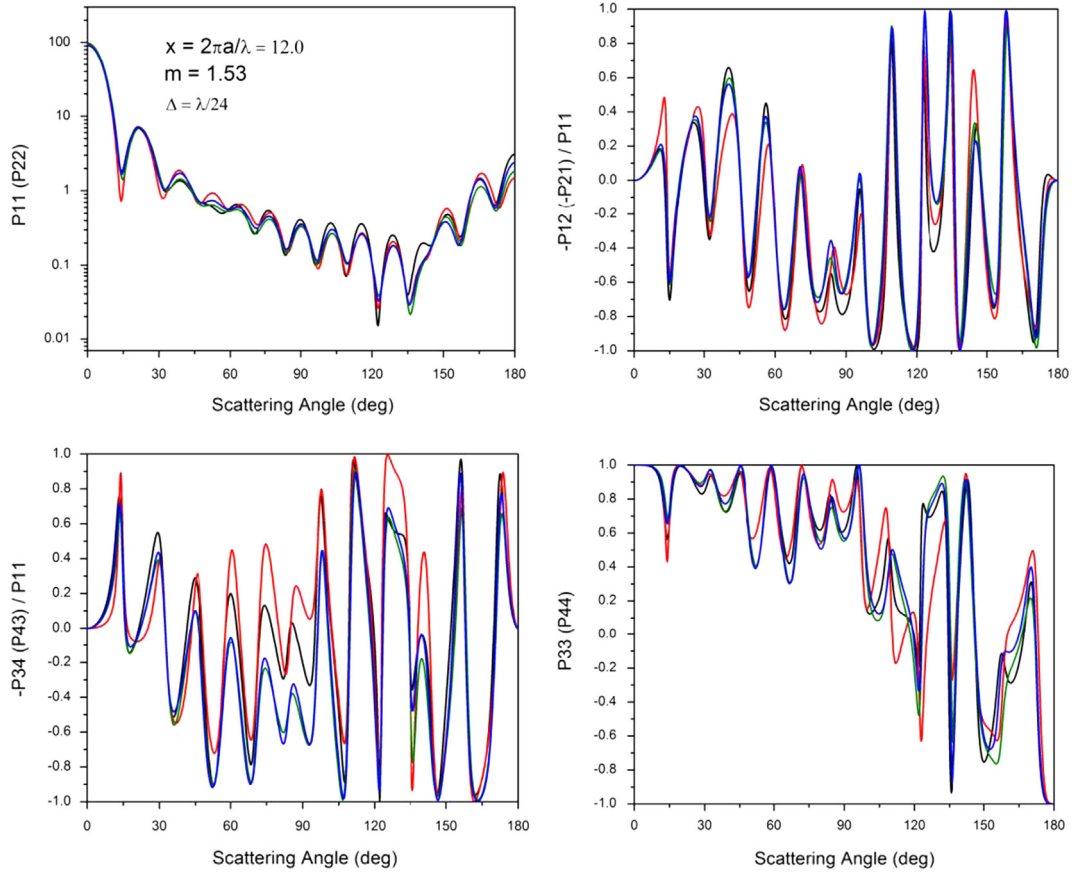


Fig. 6. Same as in Fig. 4, but in the PSTD and FDTD calculations, the spatial cell size is set as 1/24 incident wavelength.

Table 1

Light scattering efficiencies  $Q_s$  and asymmetry factors  $g$  of a spherical particle with a size parameter  $x=6$  and a refractive index  $m=1.53$  for the cases in Figs. 1–3. Also shown are the relative errors of the FDTD, PSTD, and the PSTD with wavenumber truncation (PSTD<sup>T</sup>).

	$Q_s$	$g$
Lorenz–Mie	2.456	0.581
FDTD ( $\Delta=\lambda/8$ )	1.801 (–26.6%)	0.407 (–29.9%)
FDTD ( $\Delta=\lambda/16$ )	2.249 (–8.4%)	0.543 (–7.0%)
FDTD ( $\Delta=\lambda/24$ )	2.374 (–3.3%)	0.561 (–3.5%)
PSTD ( $\Delta=\lambda/8$ )	2.359 (–3.9%)	0.590 (1.5%)
PSTD <sup>T</sup> ( $\Delta=\lambda/8$ )	3.213 (30.8%)	0.613 (5.5%)
PSTD ( $\Delta=\lambda/16$ )	2.554 (4.0%)	0.594 (2.2%)
PSTD <sup>T</sup> ( $\Delta=\lambda/16$ )	2.243 (–8.7%)	0.594 (2.2%)
PSTD ( $\Delta=\lambda/24$ )	2.502 (1.9%)	0.587 (1.0%)
PSTD <sup>T</sup> ( $\Delta=\lambda/24$ )	2.409 (–1.9%)	0.585 (0.7%)

transformations make its CPU time requirement still comparable to a FDTD calculation with finer spatial cells. For example, our test shows that for a computational domain of  $128 \times 128 \times 128$  spatial cells, the PSTD algorithm needs about 10 times CPU time that the FDTD requires for the simulation. This means that even if the PSTD simulation is done on a rougher spatial grid like  $64 \times 64 \times 64$  spatial cells, the CPU time needed in the PSTD calculation is still larger than that required by the FDTD for the  $128 \times 128 \times 128$  spatial cells. Note here that the FDTD

Table 2

Same as in Table 1, but for a spherical particle with a size parameter  $x=12$ .

	$Q_s$	$g$
Lorenz–Mie	2.549	0.651
FDTD ( $\Delta=\lambda/8$ )	1.637 (–35.7%)	0.643 (–1.2%)
FDTD ( $\Delta=\lambda/16$ )	2.209 (–13.3%)	0.695 (6.7%)
FDTD ( $\Delta=\lambda/24$ )	2.483 (–2.5%)	0.656 (0.7%)
PSTD ( $\Delta=\lambda/8$ )	2.193 (–13.9%)	0.654 (0.5%)
PSTD <sup>T</sup> ( $\Delta=\lambda/8$ )	2.695 (5.7%)	0.715 (9.8%)
PSTD ( $\Delta=\lambda/16$ )	2.585 (1.4%)	0.673 (3.4%)
PSTD <sup>T</sup> ( $\Delta=\lambda/16$ )	2.209 (–13.3%)	0.636 (–2.3%)
PSTD ( $\Delta=\lambda/24$ )	2.580 (1.2%)	0.674 (3.5%)
PSTD <sup>T</sup> ( $\Delta=\lambda/24$ )	2.574 (1.0%)	0.700 (7.5%)

and PSTD were systematically compared with the DDA for light scattering simulations, although the FDTD and PSTD were not compared directly in [30,31].

#### 4. Conclusions

In this study, a scattered-field finite-difference time domain (FDTD) and a scattered-field pseudo-spectral time domain (PSTD) model are developed for light scattering by arbitrarily shaped dielectric aerosols. The convolutional perfectly matched layer (CPML) absorbing boundary condition (ABC) is used to truncate the computational domain.

Because the scattered-field FDTD/PSTD equations include incident wave source terms, the FDTD/PSTD model allows for the inclusion of an arbitrarily incident wave source, including a plane parallel wave or a Gaussian beam like those emitted by lasers usually used in laboratory particle characterizations, etc. Numerical results show that single-scattering properties of spherical particles from the scattered-field CPML FDTD are close to those from Lorenz–Mie theory only when small spatial cell sizes are used. However, the PSTD can produce more accurate results when spatial cell size is large. As a trade-off for numerical stability, truncation of wavenumbers in the inverse Fourier transformation in the PSTD can cause significant errors in the calculated single-scattering properties of aerosols, especially in scattering efficiencies. Same as the FDTD, the PSTD has no preference to a particle shape, though different particle shapes can numerically cause some difference in results due to the imperfect ABC and Gibbs effect. Examples of application of the PSTD to nonspherical particles can be found in [18].

The PSTD can be a good algorithm for coarse-mode aerosols that requires much less computing memory, though two Fourier transformations and a power of 2 elements required by the fast Fourier transform make its CPU time requirement still comparable to a FDTD calculation which requires fine spatial cubic cells. Therefore, depending on the computer's available memory and CPU, the FDTD method could be applied for small aerosol particles, and for larger particles the PSTD method can be used. Employing the advantages of both methods, single-scattering properties of arbitrarily shaped aerosol particles can be calculated over broad size and wavelength spectra.

## Acknowledgment

This work was supported by NASA Glory fund 09-GLORY09-0027. The authors thank Michael I. Mishchenko and Hal B. Maring for support on this work.

## References

- [1] Mishchenko MI, Cairns B, Kopp G, Schueler CF, Fafaul BA, Hansen JE, et al. Accurate monitoring of terrestrial aerosols and total solar irradiance: introducing the Glory mission. *Bull Am Meteorol Soc* 2007;88:677–91.
- [2] Mie G. Beiträge zur Optik trüber Medien, speziell kolloidaler Metallösungen. Leipzig, *Ann Phys* 1908;330:377–445.
- [3] Mishchenko MI, Travis LD, Mackowski DW. T-matrix computations of light scattering by nonspherical particles. A review. *J Quant Spectrosc Radiat Transfer* 1996;55:535–75.
- [4] Singham SB, Salzman GC. Evaluation of the scattering matrix of an arbitrary particle using the coupled dipole approximation. *J Chem Phys* 1986;84:2658–67.
- [5] Draine BT, Flatau PJ. Discrete dipole approximation for scattering calculations. *J Opt Soc Am A* 1994;11:1491–9.
- [6] Piller NB, Martin OJF. Increasing the performance of the coupled-dipole approximation: a spectral approach. *IEEE Trans Antennas Propag* 1998;46:1126–37.
- [7] Yurkin MA, Min M, Hoekstra AG. Application of the discrete dipole approximation to very large refractive indices: filtered coupled dipoles revived. *Phys Rev E* 2010;82:036703.
- [8] Yurkin MA, De Kanter D, Hoekstra AG. Accuracy of the discrete dipole approximation for simulation of optical properties of gold nanoparticles. *J Nanophotonics* 2010;4:041585.
- [9] Yee KS. Numerical solution of initial boundary value problems involving Maxwell's equation in isotropic media. *IEEE Trans Antennas Propag* 1966;AP-14:302–7.
- [10] Taflove A, Brodwin ME. Numerical solution of steady-state electromagnetic scattering problems using the time-dependent Maxwell's equations. *IEEE Trans Microwave Theory Tech* 1975;MTT-23:623–30.
- [11] Taflove A. *Computational electrodynamics: the finite-difference time domain method*. Boston: Artech House; 1995.
- [12] Yang P, Liou KN. Finite-difference time domain method for light scattering by small ice crystals in three-dimensional space. *J Opt Soc Am A* 1996;13:2072–85.
- [13] Sun W, Fu Q, Chen Z. Finite-difference time-domain solution of light scattering by dielectric particles with a perfectly matched layer absorbing boundary condition. *Appl Opt* 1999;38:3141–51.
- [14] Sun W, Loeb NG, Fu Q. Finite-difference time domain solution of light scattering and absorption by particles in an absorbing medium. *Appl Opt* 2002;41:5728–43.
- [15] Taflove A, Hagness SC. *Computational electrodynamics: the finite-difference time domain method*. Boston: Artech House; 2005.
- [16] Sun W, Pan H, Videen G. General finite-difference time-domain solution of an arbitrary EM source interaction with an arbitrary dielectric surface. *Appl Opt* 2009;48:6015–25.
- [17] Liu QH. The PSTD algorithm: a time-domain method requiring only two cells per wavelength. *Microwave Opt Technol Lett* 1997;15:158–65.
- [18] Liu QH. Large-scale simulations of electromagnetic and acoustic measurements using the pseudospectral time-domain (PSTD) algorithm. *IEEE Trans Geosci Remote Sens* 1999;37:917–26.
- [19] Lee TW, Hagness SC. Pseudospectral time-domain methods for modeling optical wave propagation in second-order nonlinear materials. *J Opt Soc Am B* 2004;21:330–42.
- [20] Zhao G, Liu QH. The 3-D multidomain pseudospectral time-domain algorithm for inhomogeneous conductive media. *IEEE Trans Antennas Propag* 2004;52:742–9.
- [21] Tseng SH, Taflove A, Maitland D, Backman V. Pseudospectral time-domain simulations of multiple light scattering in three-dimensional macroscopic random media. *Radio Sci* 2006;41:RS4009, <http://dx.doi.org/10.1029/2005RS003408>.
- [22] Chen G, Yang P, Kattawar GW. Application of the pseudospectral time-domain method to the scattering of light by nonspherical particles. *J Opt Soc Am A* 2008;25:785–90.
- [23] Liu C, Panetta RL, Yang P. Application of the pseudospectral time-domain method to compute particle single-scattering properties for size parameters up to 200. *J Quant Spectrosc Radiat Transfer* 2012;113:1728–40.
- [24] Roden JA, Gedney SD. Convolutional PML (CPML): an efficient FDTD implementation of the CFS-PML for arbitrary media. *Microwave Opt Technol Lett* 2000;27:334–9.
- [25] Berenger JP. A perfectly matched layer for the absorption of electromagnetic waves. *J Comp Phys* 1994;114:185–200.
- [26] Gedney SD. An anisotropic perfectly matched layer absorbing media for the truncation of FDTD lattices. *IEEE Trans Antennas Propag* 1996;44:1630–9.
- [27] Orzag S. Comparison of pseudospectral and spectral approximations. *Stud Appl Math* 1972;51:253–9.
- [28] Gazdag J. Numerical convective schemes based on accurate computation of space derivatives. *J Comp Phys* 1973;13:100–13.
- [29] Press WH, Teukolsky SA, Vetterling WT, Flannery BP. *Numerical recipes in Fortran 77. The art of scientific computing*. 2nd ed. Cambridge, United Kingdom: Cambridge University Press; 1992 (ISBN 0-521-43064-X).
- [30] Yurkin MA, Hoekstra AG, Brock RS, Lu JQ. Systematic comparison of the discrete dipole approximation and the finite difference time domain method for large dielectric scatterers. *Opt Express* 2007;15:17902–11.
- [31] Liu C, Bi L, Panetta RL, Yang P, Yurkin MA. Comparison between the pseudo-spectral time domain method and the discrete dipole approximation for light scattering simulations. *Opt. Express* 2012;20:16763–76.

1 DEFENSE TECHNICAL  
(PDF) INFORMATION CTR  
DTIC OCA

2 DIRECTOR  
(PDF) US ARMY RESEARCH LAB  
RDRL CIO LL  
IMAL HRA MAIL & RECORDS MGMT

4 DIRECTOR  
(PDFS) US ARMY RESEARCH LAB  
RDRL CIE S  
T DEFELICE  
P CLARK  
G VIDEEN  
C WILLIAMSON